Turkish Journal of Earth Sciences

Volume 33 | Number 7 Article 4

11-12-2024

Processing of pinger, Chirp, boomer, and parametric subbottom profiler datasets

ASLIHAN NASIF

TÜBİTAK

Turkish Journal of Earth Sciences

http://journals.tubitak.gov.tr/earth/

Research Article

Turkish J Earth Sci
(2024) 33: 729-745

doi:10.55730/1300-0985.1941

Processing of pinger, Chirp, boomer, and parametric subbottom profiler datasets

Aslıhan NASIF*
Institute of Marine Sciences and Technology, Dokuz Eylül University, İzmir, Turkiye

Received: 09.08.2024 • **Accepted/Published Online:** 11.10.2024 • **Final Version:** 12.11.2024

Abstract: Subbottom profiler (SBP) systems are commonly employed for geohazard analysis in offshore engineering studies. The joint analysis of multichannel seismic and SBP data also provides additional information for analyzing submarine fluid-flow structures in shallow sediments. Detailed geohazard analyses aim to reveal small-scale changes in the seafloor and the underlying structures. Therefore, the horizontal and vertical resolution of SBP data is a crucial parameter and obtaining the necessary resolution requires appropriate data processing. This study analyzes the steps and parameters applied in processing pinger, Chirp, boomer, and parametric SBP data to determine an optimal data processing flow and parameters. Compared to multichannel seismics, the most significant challenge in processing SBP data is to suppress noise and increase the signal-to-noise ratio. Band-pass filtering is effective in eliminating swell noise, especially for boomer data. Spiking deconvolution has the most significant impact on reducing the ringy character, particularly for Chirp data. Only boomer data required the removal of multiple reflections, and predictive deconvolution was applied to eliminate the multiples. The heave effect was corrected by applying manually picked residual static values of the seafloor to the SBP data. From spectral analysis results, the wavelength of the signal was calculated, and it was observed that the parametric SBP system had the highest vertical resolution. Applications demonstrated that among the four different SBP data types, the parametric SBP data required the fewest processing steps and least time, which indicates that the parametric SBP system is the most effective in distinguishing the SBP signal from ambient noise during acquisition.

Key words: Pinger, Chirp, boomer, parametric subbottom profiler, seismic data processing, ultrahigh-resolution seismic

1. Introduction

High-resolution single-channel seismic systems that use signals in the frequency range of 2–10 kHz are generally referred to as subbottom profilers (SBPs). SBPs provide real-time high-resolution seismic reflection profiles of the seafloor and shallow subsurface sediments. A typical SBP system consists of a transceiver unit, a transducer array (excluding boomer systems), and a recording unit (Dondurur, 2018). The signal is typically generated and detected by the same transducers and raw SBP data are considered as zero-offset seismic data (Cunha and Neto, 2021).

The signal, typically at a frequency of 3.5 or 5 kHz, is produced using piezoelectric ceramic elements called transducers in the water. These elements transform electrical energy to sound signals in the sea water and vice versa. Units consisting of one or more transducers are either mounted on the hull of the ship (hull-mounted SBP systems), temporarily mounted at the side of the ship (over-the-side SBP systems), or towed at depth on a tow-fish (deep-tow SBP systems). Additionally, they can be mounted on Autonomous Underwater Vehicles and Remotely Operated Vehicles (Cunha and Neto, 2021).

The penetration of SBP signals depends on different factors such as source power, signal frequency, and pulse length as well as sediment type. It is lower in hard and compact coarse-grained sediments but can reach up to 80 m in soft and loose muddy sediments (Saleh and Rabah, 2016; Cunha and Neto, 2021). The horizontal resolution of SBP systems varies depending on the ping rate (related to the water depth) and vessel speed. Depending on the frequency of the signal used, many SBP systems achieve vertical resolutions better than 50 cm. There is a trade-off between resolution and signal penetration, where high-frequency systems provide higher vertical resolution while low-frequency systems achieve greater penetration.

SBP systems have various applications in dredging operations in ports and channels, offshore wind farm settlements, selection of submarine pipeline routes, positioning of drilling platforms, underwater archaeology, and exploration of minerals like sand or gravel in shallow waters (e.g., Schock et al., 1989; Orange et al., 2005; Quinn, 1998; Dyer, 2011; Morelli et al., 2011; Wu et al., 2020; Denich et al., 2021; Nasıf and Dondurur, 2021). SBP systems are also capable of detecting gas accumulations

* Correspondence: aslihan.nasif@deu.edu.tr

in shallow sediments and gas seeps into the water column (e.g., Dondurur et al., 2011; Vardar and Alpar, 2016). Studies on seafloor sediment reflectivity and absorption as well as sediment classification can also be conducted using SBP data (Bull et al., 1998; Stevenson et al., 2002; Theuillon et al., 2008).

There are four main types of SBP systems depending on the shape of the acoustic signal employed and the type of equipment generating the signal (Mosher and Simpkin, 1999; Dondurur, 2018): (i) single-frequency (pinger) systems, (ii) Chirp systems using sweep frequencies, (iii) boomer systems using mechanical plates, and (iv) parametric SBP systems. Pingers are linear systems that use one or more transducers to generate acoustic signals in the water, which consist of sinusoidal wave trains at fixed frequencies. These systems emit acoustic signals composed of a single-frequency component with a specific length, windowed in the frequency domain (Figure 1a). Windowing is a necessary process to obtain a pinger signal with suppressed side lobes in the time domain. The produced frequency is dependent on the resonant frequency of the piezoelectric crystal used in the transducer and is typically 3.5 or 5 kHz (Dondurur, 2018). The transducer acts as both the source and receiver. Pinger systems have several advantages, such as ease of use and maintenance, portability, and the ability of high ping rates. However, the disadvantages of single-frequency systems include a narrow frequency band, resulting in a long signal with numerous oscillations that reduces resolution, low output power (typically 10–60 J), and limitations in penetration due to high-frequency constraints. Chirp SBP systems address some of these issues.

Chirp SBP systems utilize frequency-modulated sweep signals generated by computers with predetermined signal parameters (Figure 1b). They generally operate at frequencies of 2–7 kHz with a relatively long pulse length (typically 16 or 32 ms), which increases the overall energy that can be output by the source, improving the signal penetration. The Chirp signal starts from a low frequency and gradually increases over time, typically windowed with a Blackman–Harris window, as illustrated in Figure 1b. Chirp SBP data have a unique signal shape, requiring specific data processing steps for their analysis (Bull et al., 1998; Quinn et al., 1998; Gutowski et al., 2002; Shin et al., 2022).

Boomer SBP systems, on the other hand, utilize an induction coil and a metal plate to generate an acoustic signal across a range of approximately 400 Hz to 9 kHz (Figure 1c; Denich et al., 2021). The stored energy in capacitors is discharged through an electrical wire coil, magnetically coupled to an aluminum plate behind a rubber diaphragm, producing a high-frequency seismic signal (Zheng et al., 2023) with output power ranging from 100 to 5000 J. Boomer sources are typically mounted on a catamaran towed behind a vessel.

Large transducer arrays are required for a narrow beam in linear SBP frequency bands. Nonlinear parametric SBP systems are used to overcome this problem, which can be used to produce a narrow beam with relatively small-size transducers. Two high-frequency acoustic signals called primary frequencies (e.g., f_1 = 100 kHz and f_2 = 105 kHz) are emitted into the water column simultaneously by parametric SBP systems (Figure 1d). The nonlinear interference of these two signals produces new frequencies at $2f_1$, $2f_2$, and $|f_1 \pm f_2|$. The most interesting one is $|f_1 - f_2|$ (in this case, 5 kHz), referred to as the secondary frequency (Wunderlich and Müller, 2003). Since this narrow secondary signal has no side lobes and does not oscillate, its resolution is very high (Dondurur, 2018).

In marine research, the joint interpretation of datasets with different penetration and resolution characteristics contributes to achieving the most accurate geological results (Labaune et al., 2005; Orange et al., 2005; Bellefleur et al., 2006; Mangipudi and Goli, 2014; Yang et al., 2022). For instance, while multichannel seismic data provide information about deep stratigraphy, details about shallow stratigraphy, small-offset faults, and the recent activity of faults can be obtained from high-resolution SBP data, particularly for detailed geohazard analysis. Therefore, proper processing of high-resolution SBP data is essential for revealing detailed subsurface geological structures. Specific SBP data types may require different parameters and processing techniques, which should be determined carefully. In this study, we focus on the processing of four different SBP data types, which may require different processing steps and parameters.

Previous studies of SBP data processing have typically focused on specific issues encountered during the processing of the SBP data, generally aiming to enhance the vertical resolution (e.g., Cunha and Neto, 2021; Denich et al., 2021) or compare the data from two different SBP systems (Kuhn and Michael, 1993; Vesnaver and Baradello, 2023). In addition, most studies have considered only a single SBP system, particularly focusing on Chirp SBP data processing (e.g., Quinn et al., 1998; Baradello, 2014; Kim et al., 2017). In this study, however, the necessary processing steps for four different types of SBP data are analyzed and the parameters required to obtain high-resolution output are provided.

Many data processing steps applied to SBP data are similar to those used in multichannel seismic data processing. However, there are some differences in processing high-resolution seismic data collected with different SBP systems. The aim of this study is to elucidate the details of processing pinger, Chirp, boomer, and parametric SBP datasets and to establish an appropriate data processing flow for the optimal processing of these four different types of SBP data. The scope of the study

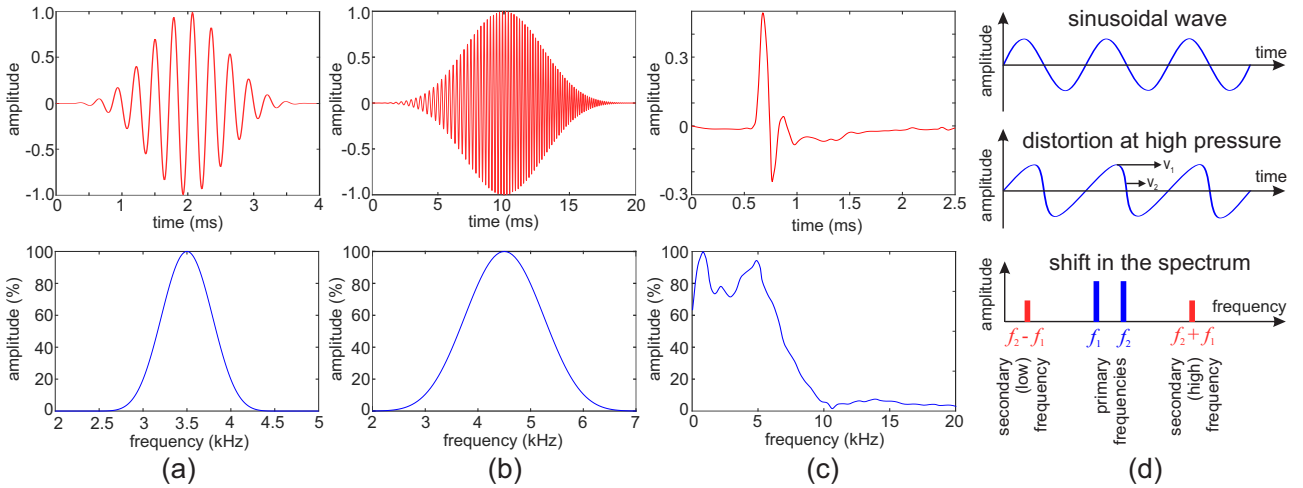

Figure 1. (a) Windowed 3.5-kHz pinger waveform (top) and its amplitude spectrum (bottom), (b) Chirp signal waveform of 2–7 kHz (top) and its amplitude spectrum (bottom), (c) boomer waveform (top) and its amplitude spectrum (bottom), and (d) signal forming in parametric SBP system (from Wunderlich and Müller, 2003).

includes the analysis of steps and parameters applied in processing different types of SBP data, which have distinct physical foundations and data characteristics.

2. Data

In this study, appropriate datasets for processing pinger, Chirp, boomer, and parametric SBP data were compiled from different regions. Pinger data were collected from Gülbahçe Bay in the Aegean Sea using the SeaBed 3010 pinger operating at 4.5 kHz (Figure 2a). Chirp data were also from the Aegean Sea, obtained in the Gulf of İzmir with the Bathy 2010 Chirp system, which uses a sweep signal of 2–7 kHz centered at 3.5 kHz (Figure 2b). Boomer SBP data were collected from offshore east-central Florida using a 100-J boomer plate that generates a signal with a center frequency of approximately 1000 Hz (Figure 2c). The parametric SBP dataset was acquired from Eckernförde Bay in eastern Germany using the SES 2000 system with a frequency of 6 kHz (Figure 2d). The data acquisition parameters of the datasets used in this study are shown in Table 1.

3. Processing SBP data

The processing of SBP data is not as complex as the processing of multichannel seismic data and generally consists of some fundamental processing steps. These steps include delay time correction, band-pass filtering, gain applications, and envelope calculations. To eliminate the ringy appearance of reflections due to the long duration of the signal with single-frequency pinger systems, spiking deconvolution is sometimes applied to the data. While some data processing steps are similar for all four different SBP datasets, the processing workflow and parameters vary depending on the characteristic features of different datasets. Figure 3 illustrates the data processing flow used in SBP processing in this study.

3.1. Data loading, Chirp preprocessing, and delay time correction

Regardless of the SBP data type, the first data processing step is always data loading. Loading the raw SBP data into the data processing system is known as data loading, which includes the transformation of proprietary data formats into the internal format of the data processing software. Subsequently, the loaded data are displayed and the seismic data are checked together with the header information.

SBP data, especially in deep waters, are often collected using delay times designed to be dependent on water depth. During data loading, these delay times are read from the header and they are added to the recording time of the SBP data. None of the SBP data used in this study were collected with delay times; therefore, delay time correction was not needed at this stage. As SBP data processing is done trace-by-trace, there is no need for geometry definition in the data processing stage.

The Chirp source signature is generated by the computer. The recorded Chirp reflection signal is the counterpart of the emitted signal (Stevenson et al., 2002). This signal's autocorrelation is known as a zero-phase Klauder wavelet. Recorded signals are cross-correlated with the known source signature to obtain Klauder wavelets, which have relatively higher resolutions and signal-to-noise ratios (Bull et al., 1998; Quinn et al., 1998; Gutowski et al., 2002). To facilitate interpretation, the envelope of this obtained trace is usually calculated. Many Chirp systems calculate the envelope of the data during the data collection phase and save the Chirp data as envelope traces.

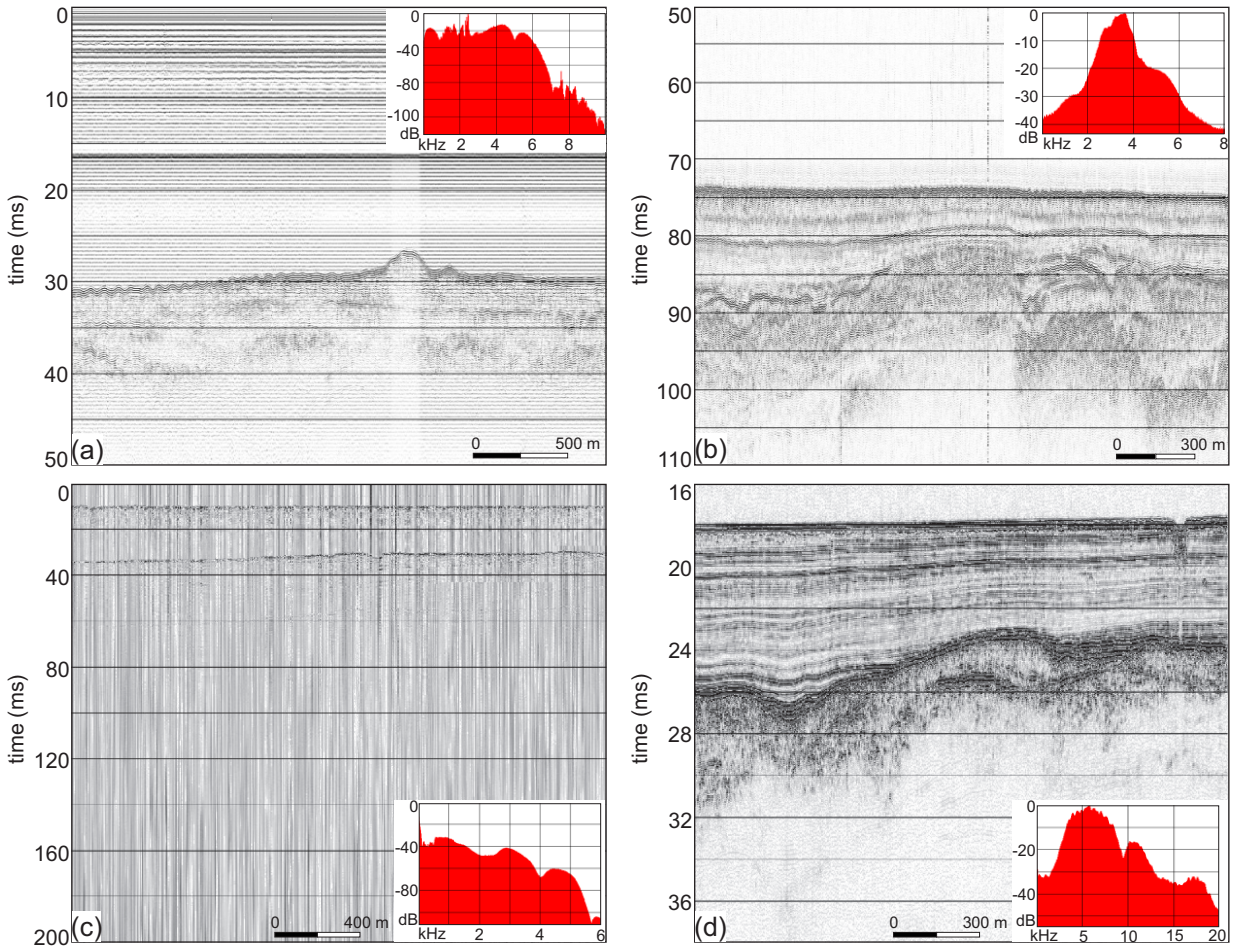

Figure 2. Raw (a) pinger, (b) Chirp, (c) boomer, and (d) parametric SBP datasets used in this study. Insets show the average amplitude spectra of the SBP data.

Table 1. Parameters of the SBP datasets used in this study.

Parameter	Pinger	Chirp	Boomer	Parametric
System	SeaBed 3010	Bathy 2010	Applied Acoustics CSP 300	SES 2000
Source depth	3 m	3 m	0.5 m	4 m
Offset	None	None	10 m	None
Sampling rate	0.05 ms	0.066 ms	0.05 ms	0.02 ms
Record length	250.0 ms	132.0 ms	200.0 ms	55.5 ms
Delay time	None	None	None	None
No. of traces	750	1400	2800	2200
Mount	Over-the-side	Over-the-side	Catamaran	Hull-mounted
Frequency band	4.5 kHz	2–7 kHz (sweep)	200–2500 Hz	6 kHz
Reference	Pekçetinöz et al. (2009)	Coşkun et al. (2016)	Subino et al. (2000)	Kaul et al. (2023)

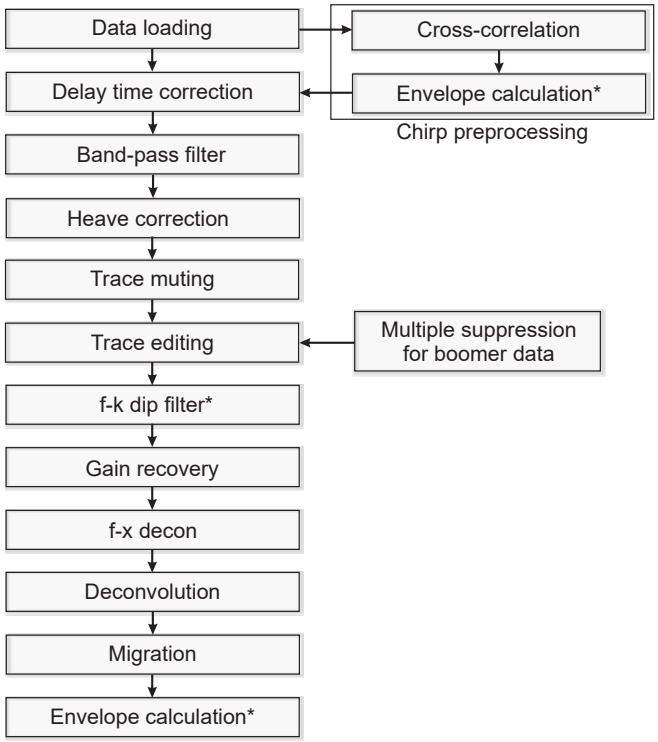

Figure 3. Data processing flow used for SBP datasets. The processing steps marked with an asterisk are optional.

3.2. Spectral analysis and band-pass filter

Following data loading, one of the first processes to be applied to SBP data is spectral analysis. This process is generally applied to all four types of SBP data. However, for boomer systems that use standard streamers for seismic signal detection, spectral analysis and band-pass filtering are particularly important. SBP data often exhibit prominent high-frequency random noise and low-frequency swell noise, and it is generally necessary to remove both high- and low-frequency components from the raw data using a band-pass filter.

In raw boomer data, the dominant noise is low-frequency swell noise, typically with a frequency band below 60 Hz. Chirp, pinger, and parametric SBP data do not exhibit a dominant swell noise component, but high-frequency random noise may be present in these data types. The Ormsby band-pass filter is used to remove low-frequency swell and high-frequency random noise from the data, which requires the determination of four frequency values to define the pass-band trapezoid (Dondurur, 2018). The first and second pair of frequencies define the transition bands of the low- (f_L) and high-frequency (f_H) cut-off bands, respectively. Both pairs of frequencies are determined from the average amplitude spectrum of the seismic data through spectral analysis (Yılmaz, 2001; Dondurur, 2018).

In Figures 4a–4d, the SBP data used in this study are presented along with their amplitude spectra after band-pass filtering. The effect of the band-pass filter process is quite evident in the pinger dataset (Figure 4a). When compared to the original data and amplitude spectra given in Figure 2, it can be observed that the band-pass filter process did not significantly improve the Chirp and parametric SBP data (Figures 4b and 4d). The genuine reflection amplitudes of both data types are concentrated in the frequency band of approximately 2–4.5 kHz for Chirp data and 1.8–9.5 kHz for parametric SBP data, and there is no prominent high-amplitude noise component outside these bands. Therefore, the cut-off values of the Ormsby band-pass filter for Chirp data are determined as f_L = 2–2.2 kHz, f_H = 4.2–4.5 kHz, and, for parametric SBP data, f_L = 1.8–2 kHz and f_H = 9.3–9.5 kHz.

The spectrum of the pinger data shows that signal amplitudes are concentrated between 2.5 and 5 kHz, and there is also a noise signal with quite high amplitudes around 2.2 kHz (Figure 2a). This noise in the spectrum is due to high-amplitude noise extending horizontally in the section at an arrival time of approximately 15 ms. With the Ormsby band-pass filter with cut-off frequencies of f_L = 2.5–2.6 kHz, f_H = 4.9–5 kHz, it is observed that a large portion of this noise is suppressed (Figure 4a). In the boomer data, however, swell noise amplitudes below 200

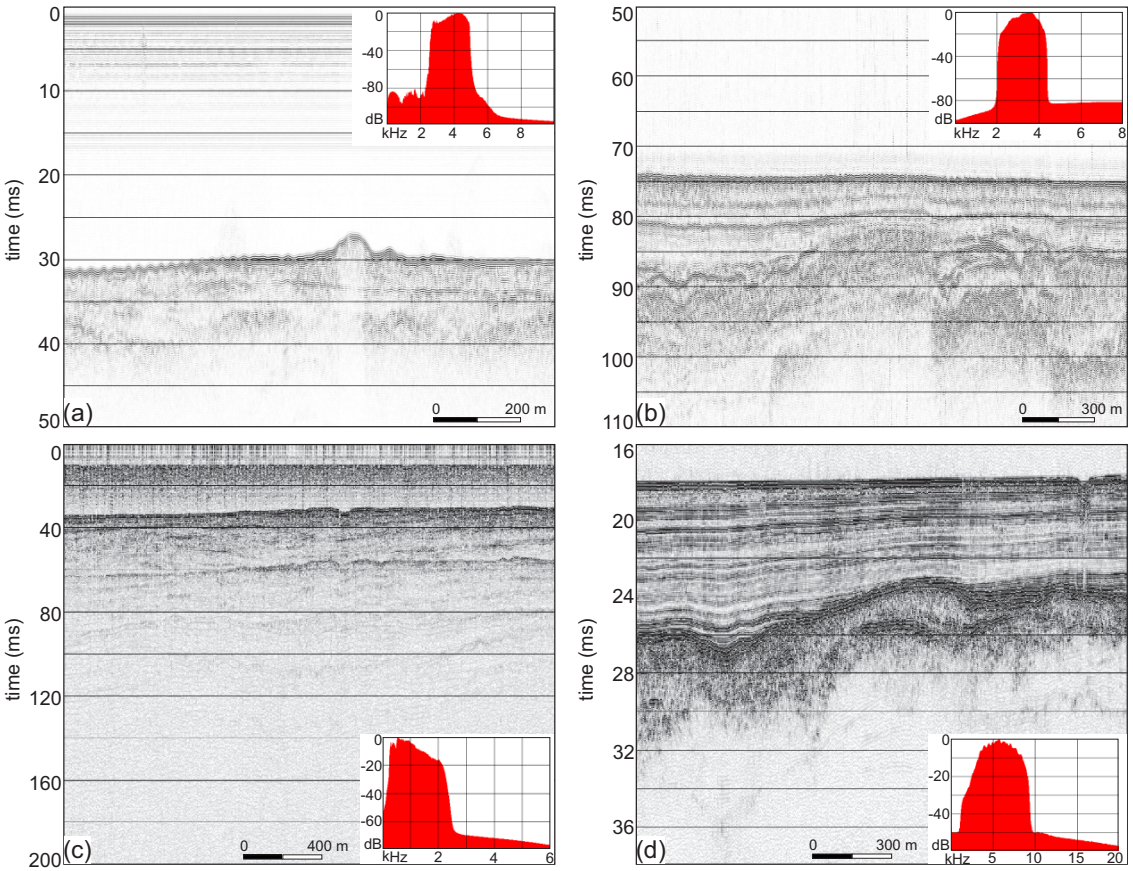

Figure 4. Band-pass filtered (a) pinger (2500–5000 Hz), (b) Chirp (2000–4500 Hz), (c) boomer (200–2500 Hz), and (d) parametric (1800–9500 Hz) SBP datasets used in this study. Insets show the average amplitude spectra of the SBP data after band-pass filtering.

Hz are quite dominant. The notch frequency, due to ghost-reflection interference, appears around 2500 Hz (Figure 2c). Therefore, after applying the Ormsby band-pass filter with f_L = 200–300 Hz and f_H = 2.3–2.5 kHz to boomer data, reflections become quite prominent (Figure 4c).

3.3. Heave correction

SBP data, using higher frequencies than conventional seismics and much higher ping (and hence trace) intervals, are strongly influenced by the sea state during data acquisition. The horizontal resolution and signal-to-noise ratio of high-resolution SBP data significantly decrease when data are collected during rough weather conditions. If the swell height is greater than the vertical resolution of the SBP system, which is typically about 10 cm, the heave effect will have a disruptive impact on the SBP data (Gutowski et al., 2002; Kim et al., 2016; Shin et al., 2022). Trace-by-trace consistency can be compromised, the horizontal continuity of the reflections decreases, and reflecting interfaces become wavy. In such cases, identifying true geological events, and especially shallow structures like fault throws, is difficult.

Mitigation of the heave effect is typically performed in two steps: determining the seafloor and then correcting for the heave effect. For seafloor determination, manual picking, a maximum cross-correlation scheme, reflection amplitude of the sea-bottom approach, or use of multibeam echosounder data are recommended (Kim et al., 2017).

In this study, a significant heave effect was observed in the pinger, Chirp, and boomer datasets (Figure 5).

The process of correcting the heave effect is demonstrated for pinger data in Figure 5a. For this process, manual picking of the seafloor was first performed and then the obtained seafloor picks were smoothed (Figure 5b). The time difference between the two curves was taken as the residual static value and then applied to the SBP data as heave correction. Positive residual static values were added to the arrival times of the traces while the negative values were subtracted. After this correction, the trace-by-trace consistency of pinger (Figure 5c), Chirp (Figures 5d and 5e), and boomer (Figures 5f and 5g) data significantly improved, and the signal-to-noise ratio and lateral resolution of the data increased, especially for

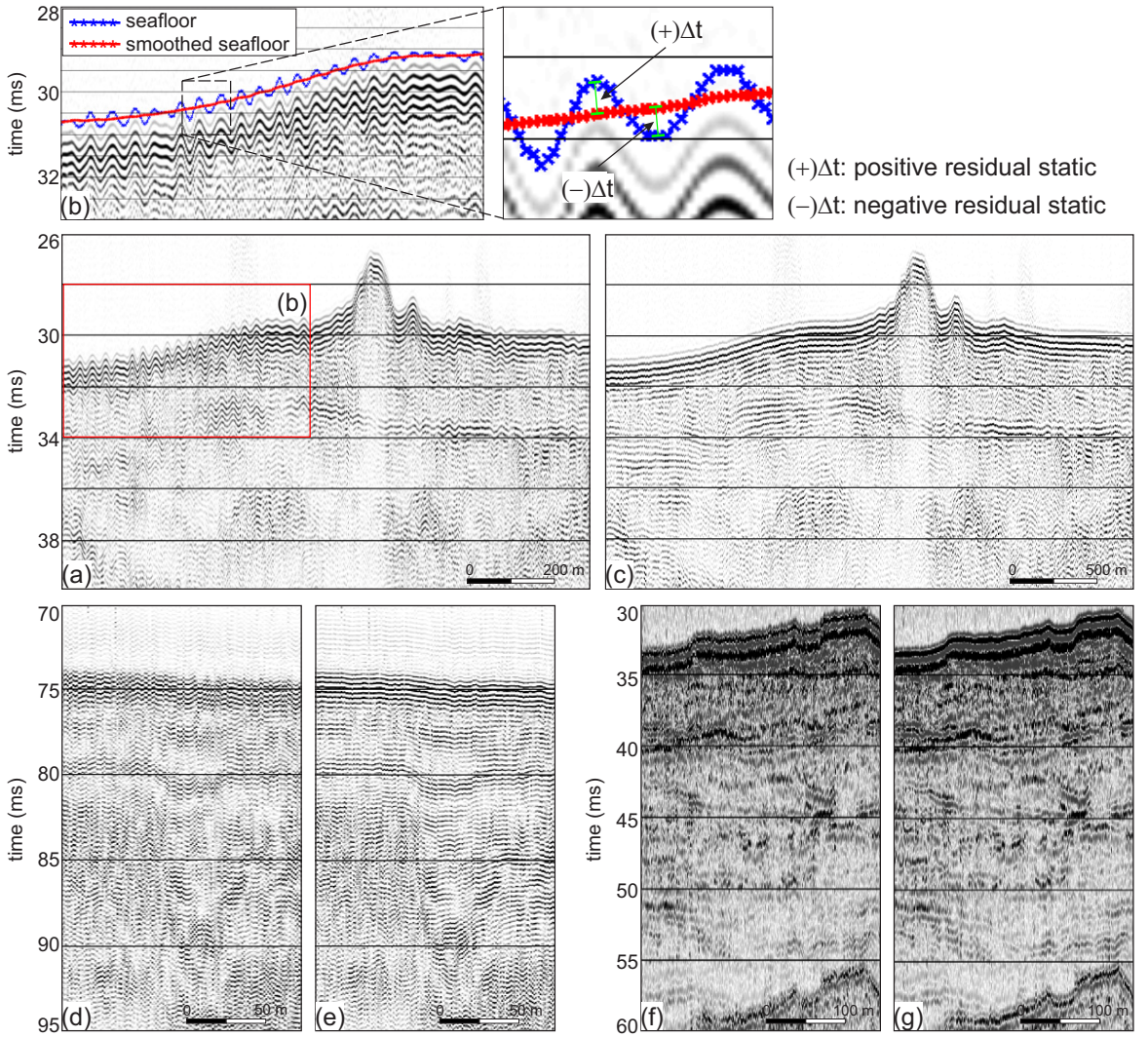

Figure 5. Heave correction process. (a) Band-pass filtered pinger data. (b) Close-up of the heave effect in (a) showing the seafloor picks (blue curve) and their smoothed version (red curve). The positive or negative time difference between two curves provides the residual static (heave correction) value. (c) Pinger data after heave correction. (d, e) A portion of Chirp data and (f, g) a portion of boomer data before and after heave correction, respectively.

early arrivals. Although the manual picking approach for calculating residual static values is a straightforward method, it strongly depends on accuracy in picking the seafloor. With more accurate and detailed seafloor picking, the heave correction will be more accurate.

3.4. Trace editing and muting

In SBP data, traces containing excessive noise and shots related to missed shots are considered unusable and are nullified by being multiplied by zero. This process, known as trace editing, is applied to different SBP datasets in a similar way, being particularly needed for boomer data. Figure 6a shows a missed shot in the boomer section (blue arrow) and Figure 6b shows the result of removing that trace through the trace edit/kill process. Traces zeroed out after trace editing can be easily interpolated by applying a trace mix, as demonstrated in Figure 6c, depicting the interpolated version of the killed trace after a trace mix operation incorporating three adjacent traces.

The trace muting operation is generally applied as a top mute to SBP data, zeroing out all events observed in the water column in the data appearing before the seafloor reflection. The top mute process is applied to different SBP datasets in a similar way. The purpose is simply to remove the output signal for Chirp, pinger, and parametric SBP data and to remove the direct wave from boomer data, along with the noise amplitudes in the water column. Figures 6d and 6e provide an example of top mute application to pinger and boomer data. The top mute should be applied

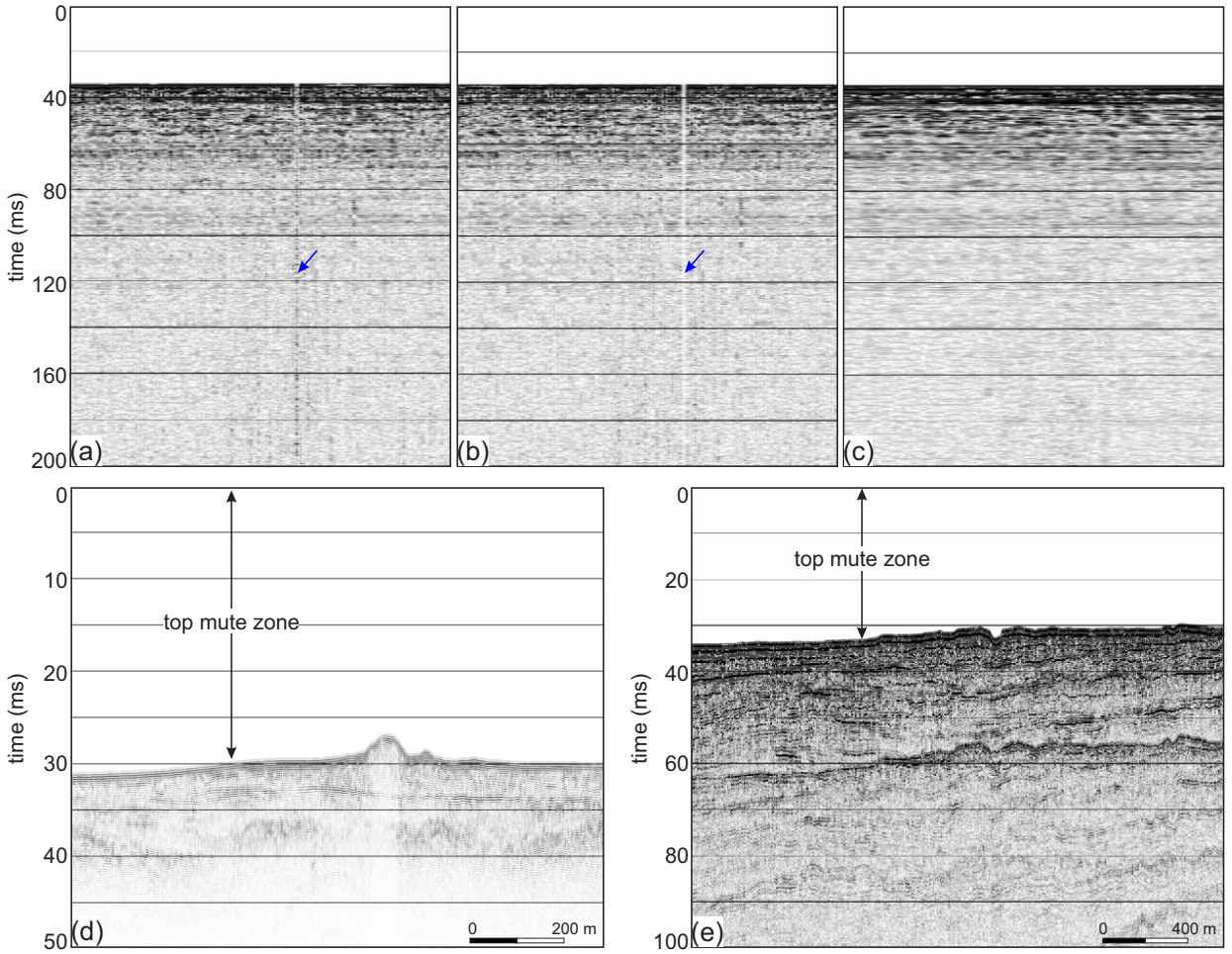

Figure 6. Examples of trace muting and trace edit/kill processes. (a) A missed shot in the boomer section (blue arrow), (b) the result of removing this trace with the trace edit/kill process, and (c) the interpolated version of the killed trace after a trace mix operation with three adjacent traces. (d) Pinger and (e) boomer data after top mute process.

carefully to the data since it may remove indications of gas flares in the water column.

3.5. f-k dip filter

In the frequency-wavenumber (f-k) domain, the process known as f-k filtering separates events with different dips that interfere in time sections and allows the removal of some associated noise by performing a 2D Fourier transform in the frequency domain. While the f-k filter is a crucial component of multichannel seismic data processing, its application to SBP data is typically optional and depends on the type and characteristics of the embedded noise components.

The f-k filter is generally not applied to Chirp and parametric SBP data. It is commonly used to suppress random noise in the late arrivals of boomer data and to enhance the resolution in deeper parts (Figure 7). Since reflections in the boomer data are generally horizontal, their amplitudes are concentrated around the zero wavenumber axis in the f-k panel (Figure 7a). The portion outside this area, enclosed by the f-k polygon, is multiplied by zero, suppressing noise amplitudes with different dips and frequencies outside the reflection amplitudes. The f-k filter is seen to enhance the reflection amplitudes, especially in the deeper parts of the boomer data (blue arrows, Figure 7b).

3.6. Gain recovery

The amplitude of seismic signals propagating through the water column and subbottom layers decreases with distance, especially due to spherical divergence and absorption effects. The reflection amplitudes in the late arrivals of SBP data are relatively small and need to be enhanced. One of the most commonly used gain control applications is automatic gain control (AGC), and the most crucial parameter to be selected for AGC applications is

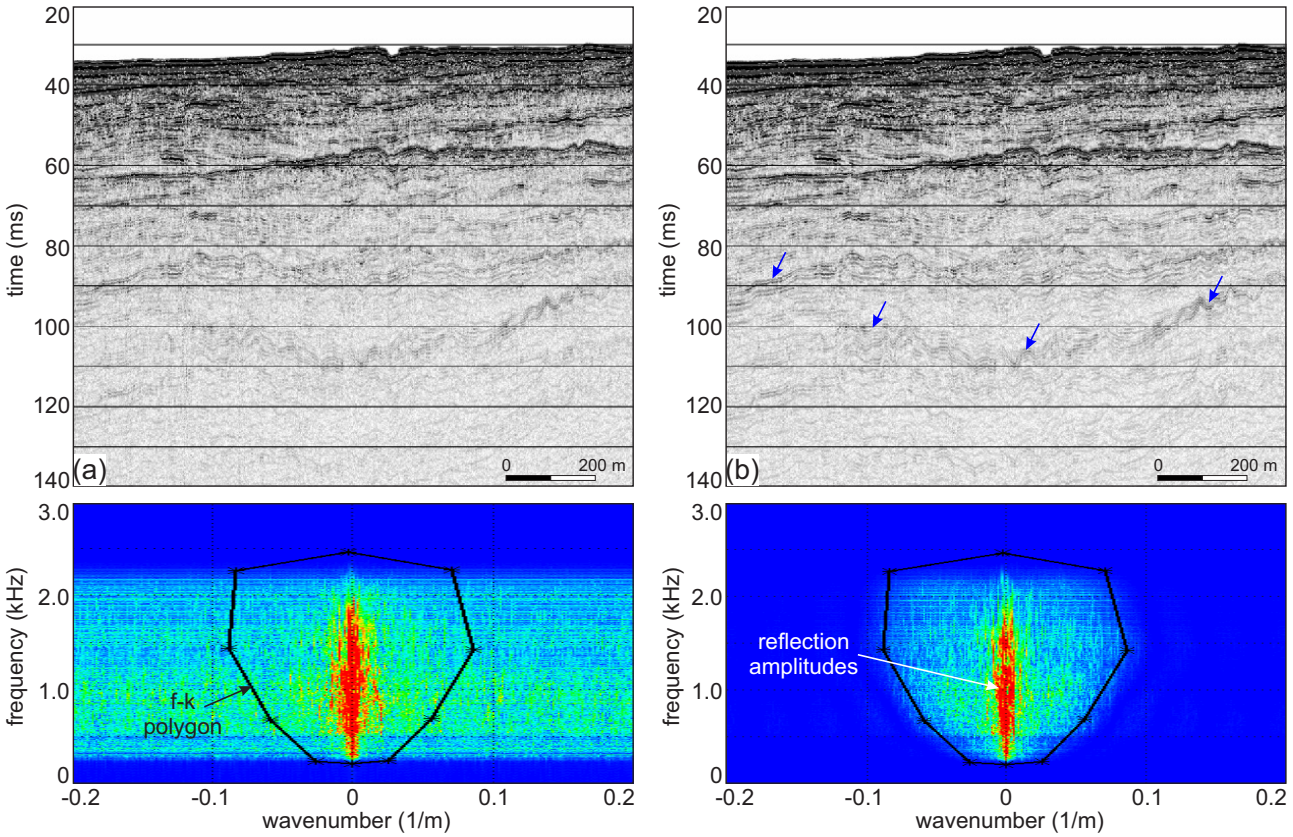

Figure 7. Application of the f-k filter to boomer SBP data. Boomer data (a) before and (b) after the f-k filter. Blue arrows show the increased amplitudes of the primary reflections after filtering. Corresponding f-k spectra of the data are presented below the sections.

the window length. As the window length decreases, the amplitudes in both shallow and deep regions of the data become more balanced. In practice, the appropriate window length is chosen based on the recording length of the input data. Since the recording length for SBP data is much shorter compared to conventional seismics, relatively shorter AGC window lengths should be preferred. One disadvantage of AGC is that it removes trace-by-trace relative amplitude variations, which may be an important parameter for the exploration of gassy sediments. Therefore, AGC gain is typically used for display purposes for seismic data during the processing phase.

Figure 8 illustrates the results of applying AGC gain to the SBP datasets used in this study. AGC with an operator length of 25 ms was applied to the pinger data, 50 ms to the Chirp and boomer data, and 5 ms to the parametric SBP data. Compared to the sections in Figure 4 with no gain, high amplitudes in the early arrivals of the sections are suppressed while low amplitudes in the late arrivals are enhanced after the AGC process, achieving a balanced amplitude distribution throughout the entire sections of Figure 8.

3.7. f-x decon

In multichannel seismic data, stacking is the most effective method for suppressing random noise. However, in single-channel SBP data, stacking is not applicable, necessitating additional processes such as f-x decon or trace mixing to suppress random noise. In this study, f-x decon was applied to all four types of SBP data (Figure 9). The f-x decon, which enhances the lateral resolution of the data (Gülünay, 1986), is used to suppress random noise, which is particularly prominent in the late arrivals of SBP data (Quinn et al., 1998; Baradello, 2014). The horizontal window length is 4 traces for Chirp, Pinger, and parametric SBP data while it is 50 traces for boomer. Compared to the input datasets provided in Figure 8, the effectiveness of the f-x decon in suppressing random noise is evident, especially in the late arrivals of boomer and parametric SBP data (Figure 9).

3.8. Spiking and predictive deconvolution

To reduce the ringy appearance of SBP data and mitigate potential ghost-reflection effects in boomer data, spiking deconvolution is applied. Conventional Wiener–Levinson deconvolution can only be used on minimum-phase

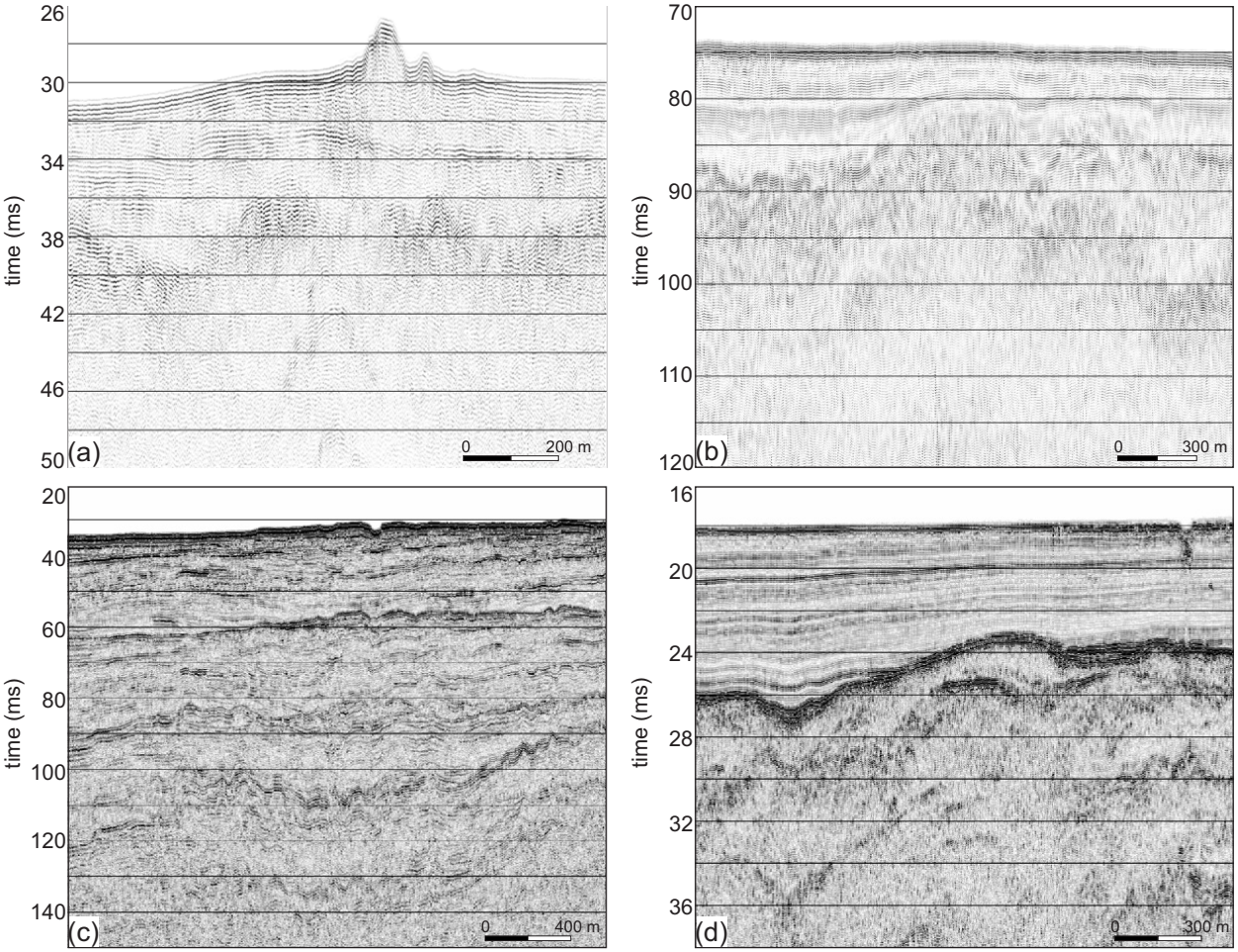

Figure 8. Gain application performed for SBP data. (a) Pinger data after 25 ms of AGC, (b) Chirp data after 50 ms of AGC, (c) boomer data after 50 ms of AGC, and (d) parametric SBP data after 5 ms of AGC.

data, making it applicable to the pinger and boomer SBP datasets. Chirp data are typically recorded and visualized in envelope form. Baradello (2014) suggested a Wiener filter to transform the sweep signal into a minimum-phase pulse, which makes Chirp data causal in applying predictive deconvolution. Denich (2021) demonstrated the theoretical feasibility of applying spiking deconvolution to Chirp data in envelope form. In this study, however, spiking deconvolution is applied to Chirp data before computing the envelope.

Figure 10 shows the results of the deconvolution process applied to the SBP data along with the average amplitude spectra of all datasets. The spiking deconvolution operator length is set to 1 ms for pinger data (Figure 10a), 2 ms for Chirp data (Figure 10b), 5 ms for boomer data (Figure 10c), and 0.5 ms for parametric SBP data (Figure 10d). From the amplitude spectra of the sections, it is evident that spiking deconvolution enhances the resolution of all four datasets. Before applying spiking deconvolution to the Chirp data, they were transformed to the minimum-phase equivalent and Wiener spiking deconvolution was applied. Compared to the SBP sections shown in Figure 9, the ringy character observed especially in the shallow reflections is eliminated after spiking deconvolution, particularly in the Chirp section (Figure 10b).

While various approaches have been developed to remove multiple reflections from seismic sections, the theories behind most of these approaches are only suitable for application to multichannel seismic data. The most suitable method for removing multiple reflections in single-channel seismic or SBP data is predictive deconvolution. In this study, multiple reflections observed in boomer data were removed using predictive deconvolution (Figure 10e). The operator length and prediction lag parameters for predictive deconvolution were determined by calculating the autocorrelation of the input data. Figures 10f and 10g show autocorrelation sections of the input boomer data before and after predictive deconvolution, respectively.

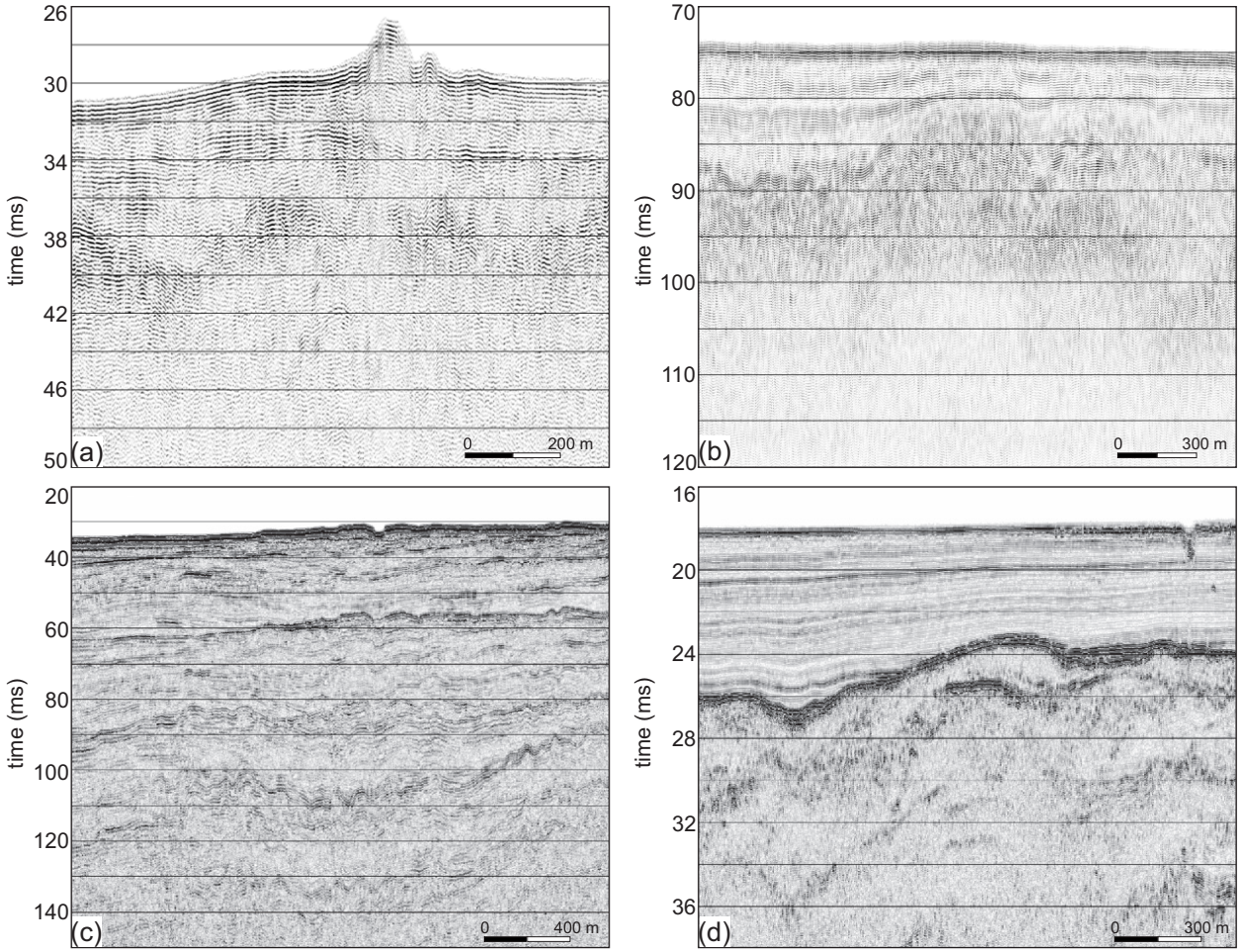

Figure 9. (a) Pinger, (b) boomer, (c) Chirp, and (d) parametric SBP data after f-x decon.

According to autocorrelation data, both the appropriate operator length and prediction lag parameters were determined to be 20 ms. Compared to the input boomer section given in Figure 10c, it can be observed that the predictive deconvolution process successfully removes the multiple reflections from the data (Figure 10e).

3.9. Migration

Migration is a process that moves reflections from dipping reflectors to their true positions in a seismic section, making the seismic section resemble the subsurface geological section. Since SBP data are zero-offset data, only poststack time migration can be applied to SBP data. All migration algorithms require information about the subsurface seismic velocity distribution. However, obtaining the subsurface velocity from single-channel seismic data is not feasible. Therefore, Stolt migration as a constant-velocity migration algorithm is applied to the SBP data in this study.

Figure 11 illustrates the SBP datasets after Stolt migration. The input sections for the migration process are shown in Figure 10. Due to their relatively low penetration, SBP data provide information about the stratigraphy in the first few tens of meters from the seafloor. In these sections, the seismic wave velocity is not significantly different from the P-wave velocity in the seawater. Therefore, a constant seismic velocity of 1500 m/s was used in the migration process.

3.10. Envelope calculations

Pinger and Chirp SBP data exhibit a ringy character due to relatively long signal periods. This implies that the reflection received from a single interface is represented by a signal with multiple oscillations in the SBP data. While not mandatory, to enhance the interpretability of the data, envelope sections are commonly calculated for pinger and Chirp datasets and interpretation is often performed using the envelope data. This is typically a routine process for Chirp data. Figure 12 displays envelope sections calculated as the final step of the data processing for pinger and Chirp SBP data. In both datasets, the main reflections became more prominent in the envelope sections, leading to increased trace-by-trace consistency.

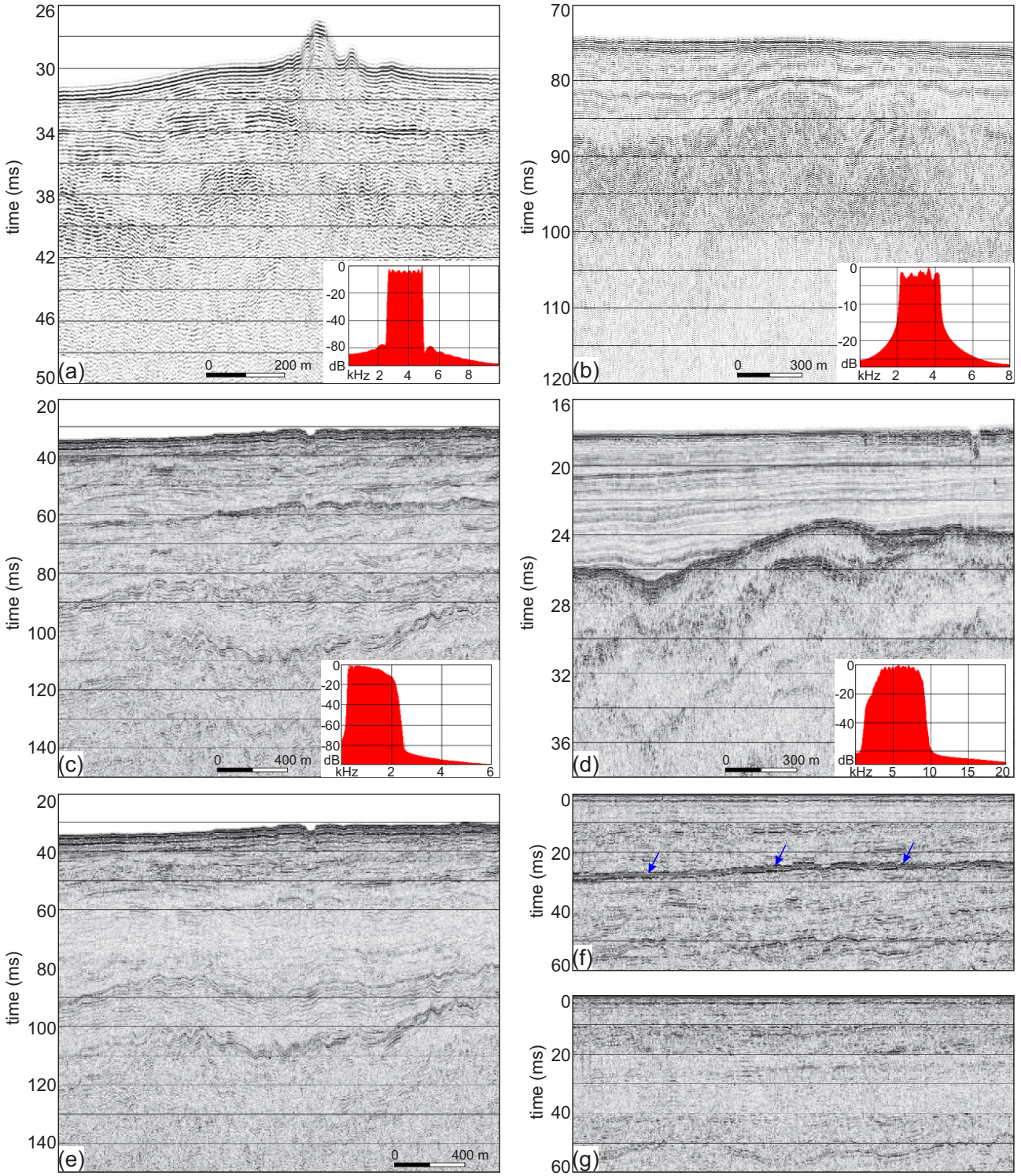

Figure 10. (a) Pinger, (b) boomer, (c) Chirp, and (d) parametric SBP sections after spiking deconvolution. Insets display the average amplitude spectra of each SBP profile. (e) Boomer data after predictive deconvolution to remove multiple reflections. Autocorrelation sections of the boomer data (f) before and (g) after predictive deconvolution. Blue arrows indicate long-period multiple-reflection amplitudes.

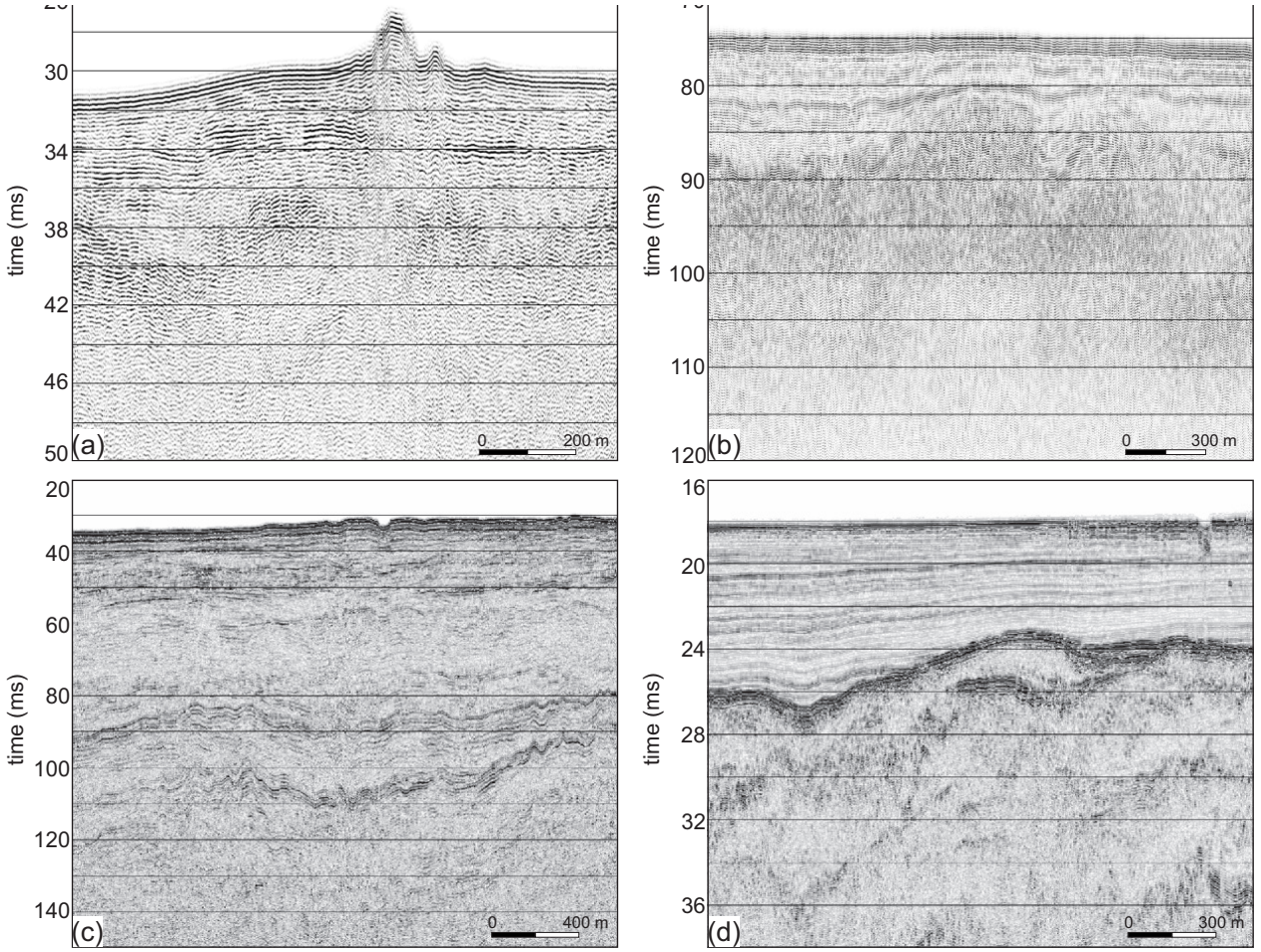

Figure 11. (a) Pinger, (b) boomer, (c) Chirp, and (d) parametric SBP sections after constant-velocity Stolt migration. Seismic velocity of 1500 m/s was used in the migration process.

4. Discussion

SBP systems are widely used in contemporary marine geoengineering studies for offshore geohazard analysis (Trabant, 1986) due to their relatively low data acquisition costs, capability of collecting data in shallow areas, ability to provide high-resolution data, and relatively easy data processing steps. Analyses conducted using these systems include investigations of small-offset active faults, slumps and slides, scarp structures, mobile seafloor sediments, submarine fluid flow, and related structures (e.g., Baraza et al., 1999; Hovland et al., 2002; Dondurur et al., 2011; Nasıf and Dondurur, 2021). Detailed geohazard analysis aims to reveal these structures and their small-scale variations beneath the seafloor. At this stage, the horizontal and vertical resolution of SBP data becomes a crucial parameter. Achieving the necessary resolution requires not only accurate data collection but also appropriate processing.

SBP data provide the shallow stratigraphic connection to deep stratigraphy information obtained by multichannel conventional seismic data. In this context, for the hydrocarbon industry, the simultaneous analysis of both multichannel seismic and high-resolution SBP data offers additional insights into the analysis of submarine fluid-flow structures in shallow areas, such as pockmarks, shallow gas accumulations, and gas chimneys (e.g., Dondurur et al., 2011; Simonetti et al., 2013). The simultaneous collection of high-resolution SBP data with multichannel seismic data is significant for reducing data acquisition costs and providing extra information that can correlate shallow and deep stratigraphy. When the signal generated by the source is suitable in terms of frequency band and data acquisition procedures, pinger, Chirp, and parametric SBP data can be collected simultaneously with multichannel seismics. However, due to the use of a streamer as a receiver in both methods and the partial overlap of signal frequency bands, it may not be feasible to collect boomer data simultaneously with multichannel seismics.

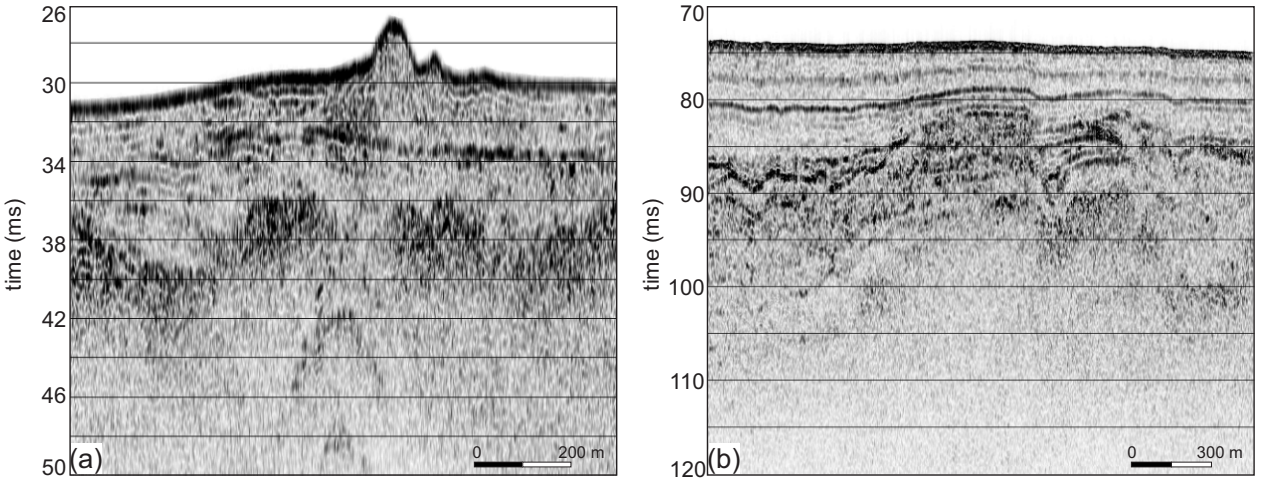

Figure 12. Envelope sections of (a) pinger and (b) Chirp SBP datasets as the final step of data processing.

The processing of SBP data, while being similar to the processing of multichannel seismic data in various ways such as band-pass filtering, gain application, and poststack migration processes, requires unique procedures and the application of different data processing parameters (Bull et al., 1998; Quinn et al., 1998; Gutowski et al., 2002; Kim et al., 2017; Shin et al., 2022; Yang et al., 2022). The applications in this study have demonstrated that among the four different SBP data types, parametric SBP data are the least demanding in terms of processing time. For instance, these data may not require preprocessing or an f-k filter. This observation indicates that the parametric system is the most effective SBP system to discriminate the SBP signal within the ambient noise during data recording. Therefore, the processing of parametric SBP data requires the least amount of processing effort and time.

According to the spectral analysis results shown in Figure 4, the dominant frequencies and resolution parameters of the SBP data used in this study are provided in Table 2. Signal wavelength λ is calculated from the relationship $\lambda = V/f_D$, where λ represents the signal wavelength (m), V is the velocity of the P wave in seawater (m/s), and f_D is the dominant frequency of the recorded signal (Hz). Accordingly, the vertical resolution of these SBP systems can be calculated taking into account the Rayleigh criterion (λ/4), as shown in Table 2 for seismic velocity of 1500 m/s. The system with the highest vertical resolution is the parametric SBP system, with vertical resolution of 6.2 cm.

Compared to multichannel seismic data, the most prominent challenge in processing SBP data arises from the need to reduce noise content and increase the signal-to-noise ratio. As the stacking process cannot be applied to SBP data, particularly in suppressing random noise, the application of the trace mix (Figure 6) and/or f-x decon (Figure 9) becomes essential. Boomer SBP data recorded using a conventional single-channel streamer contain distinctive swell noise (Figure 2). The band-pass filter is most effective on boomer SBP data, facilitating the removal of swell noise (Figure 4). Pinger, Chirp, and parametric SBP data, utilizing transducers for signal generation and perception, do not have dominant swell noise given that the frequency band of the generated signal is significantly higher than that of the swell frequency band (Figure 2).

In SBP data, the disruptive effect of heave can be observed due to rough sea conditions, reducing both the horizontal and vertical resolution of the data (Kim et al., 2017; Shin et al., 2022). It has been observed that the heave effect particularly complicates the identification of small fault throws in pinger and Chirp data and significantly reduces the signal-to-noise ratio in boomer data. In this study, the heave effect was mitigated by calculating residual static correction values obtained as the time difference between manually picked seabed times and their smoothed versions (Figure 5b). Although the process is time-consuming due to the manual picking procedure, effective results were observed for pinger, Chirp, and boomer SBP data (Figure 5). The removal of heave effect enhances trace-by-trace consistency, potentially leading to more accurate results in the autotrack application during the interpretation phase.

Spiking deconvolution, while being a crucial step in enhancing the resolution of SBP data, is a time-consuming process since it requires numerous tests to determine the appropriate operator length for application. In this study, spiking deconvolution increased the data resolution by flattening the amplitude spectrum of the data, while the most significant enhancement was observed for Chirp data since it reduced the ringy character of the shallow reflections (Figure 10). Only the boomer data required the suppression of multiple reflections, and predictive deconvolution was applied to the boomer data to remove

Table 2. Resolution parameters of the datasets used in this study for seismic velocity of 1500 m/s.

Parameter	Pinger	Chirp	Boomer	Parametric
Dominant frequency (Hz)	4500	3500	1000	6000
Signal wavelength (m)	0.3	0.4	1.5	0.25
Vertical resolution (cm)	7.5	10	37.5	6.2

multiples. The determination of operator length and prediction lag parameters is highly crucial in predictive deconvolution (Robinson and Treitel, 1967), and extensive testing is necessary for their proper selection. In cases where these parameters are not appropriately chosen, a reduction in the amplitudes of primary reflections can be observed (Güney et al., 2019).

It was further observed that Stolt migration produced reliable results for all four SBP datasets. It is a frequency-domain method, which is computationally efficient compared to time-domain methods. SBP data often involve relatively simple and shallow geologies, where the assumption of constant or near-constant velocity is reasonable. Stolt migration is optimal for such cases, as it assumes a constant migration velocity. In addition, SBP data are typically high-frequency, benefiting from the capacity of Stolt migration to maintain high-resolution detail in shallow subsurface imaging. Stolt migration is less effective in more complex geological settings where velocities vary significantly or the topography is irregular. In such cases, other migration methods, such as Kirchhoff migration, might be more appropriate. However, for the simple, shallow, and relatively homogeneous environments typical of SBP data, Stolt migration can produce good results.

5. Conclusions

SBP systems are widely utilized in assessing offshore geohazards by detecting small-scale variations in the seafloor and underlying subsurface structures. As a result, the resolution of SBP data is a critical factor, and achieving the required resolution is contingent upon effective data processing. Since the stacking process cannot be applied to SBP data for suppressing random noise, alternative techniques such as trace mixing or f-x decon become crucial to enhance the signal-to-noise ratio.

In Chirp data, spiking deconvolution effectively diminishes the characteristic ringy nature of the signal. Only boomer data required the removal of multiple reflections in the present study, which were successfully suppressed by predictive deconvolution. The heave effect was compensated by calculating residual static correction values based on the time difference between manually picked seabed times and their smoothed pinger data counterparts. This correction enhances trace-by-trace consistency and potentially improves the accuracy of autotracking during the interpretation stage.

Spectral analysis revealed that the parametric SBP system provided the highest vertical resolution after the processing. Additionally, the parametric SBP data required the least processing time, suggesting that this system is the most efficient for isolating SBP signals from ambient noise during acquisition.

It was found that Stolt migration yielded reliable results across all four SBP datasets, owing to its assumption of constant migration velocity. Given that SBP data are typically obtained at high frequencies, Stolt migration effectively preserves high-resolution details in shallow subsurface imaging.

Acknowledgment
I would like to thank Dr. Derman Dondurur for his valuable contributions and comments on the manuscript.

Declarations
Author contributions: Aslıhan Nasıf performed the conceptualization, seismic data analysis, modeling, methodology, visualization, writing, review, and editing of the manuscript.

Funding
No funding, grants, or other support was received during the preparation of this manuscript.

Employment
None.

Financial interests
The author has no relevant financial or nonfinancial interests to disclose.

Nonfinancial interests
None.

Competing interests
The author has no competing interests to declare that are relevant to the content of this article.

Data
The pinger and Chirp datasets can be provided upon request. The parametric SBP and boomer datasets are publicly available at https://doi.pangaea.de/10.1594/PANGAEA.961650?format=html#download and https://pubs.usgs.gov/ds/496/, respectively.

References

Baradello L (2014). An improved processing sequence for uncorrelated Chirp sonar data. Marine Geophysical Research 35 (4): 337–344. https://doi.org/10.1007/s11001-014-9220-1

Baraza J, Ercilla GH, Nelson C (1999). Potential geologic hazards on the eastern Gulf of Cadiz slope (SW Spain). Marine Geology 155 (1–2): 191–215. https://doi.org/10.1016/s0025-3227(98)00147-9

Bellefleur G, Duchesne MJ, Hunter J, Long BF, Lavoie D (2006). Comparison of single- and multichannel high-resolution seismic data for shallow stratigraphy mapping in St. Lawrence River estuary, Quebec. Geological Survey of Canada D2: 1-10. https://doi.org/10.4095/223015

Bull JM, Quinn R, Dix JK (1998). Reflection coefficient calculation from marine high-resolution seismic reflection (Chirp) data and application to an archaeological case study. Marine Geophysical Research 20 (1): 1–11. https://doi.org/10.1023/A:1004373106696

Coşkun S, Dondurur D, Çifçi G, Aydemir A, Drahor MG (2016). Natural and anthropogenic submarine morphologies revealed by high resolution acoustic data in the Gulf of Izmir, western Turkey. Marine and Petroleum Geology 71: 211–224. https://doi.org/10.1016/j.marpetgeo.2015.12.012

Cunha J, Neto AA (2021). Ultrahigh-resolution seismic enhancement: The use of colored inversion and seismic attributes on sub-bottom profiler data. Journal of Applied Geophysics 184: 104184. https://doi.org/10.1016/j.jappgeo.2020.104184

Denich E, Vesnaver A, Baradello L (2021). Amplitude recovery and deconvolution of Chirp and Boomer data for marine geology and offshore engineering. Energies 14 (18): 5704. https://doi.org/10.3390/en14185704

Dondurur D (2018). Acquisition and processing of marine seismic data. Elsevier. https://doi.org/10.1016/C2016-0-01591-7

Dondurur D, Çifçi G, Drahor MG, Coşkun S (2011). Acoustic evidence of shallow gas accumulations and active pockmarks in the İzmir Gulf, Aegean Sea. Marine and Petroleum Geology 28 (8): 1505–1516. https://doi.org/10.1016/j.marpetgeo.2011.05.001

Dyer JM (2011). Geohazard identification: the gap between the possible and reality in geophysical surveys for the engineering industry. Marine Geophysical Research 32 (1–2): 37–47. https://doi.org/10.1007/s11001-011-9137-x

Gülünay N (1986). FXDECON and complex wiener prediction filter. SEG Technical Program Expanded Abstracts 1986: 368-371. https://doi.org/10.1190/1.1893128

Gutowski M, Bull J, Henstock T, Dix JK (2002). Chirp sub-bottom profiler source signature design and field testing. Marine Geophysical Research 23 (5–6): 481–492. https://doi.org/10.1023/b:mari.0000018247.57117.0e

Güney R, Karslı H, Dondurur D (2019). Optimum parameter selection in offset-dependent predictive deconvolution: testing on multichannel marine seismic data. Marine Geophysical Research 40 (4): 601–617. https://doi.org/10.1007/s11001-019-09390-w

Hovland M, Gardner JV, Judd AG (2002). The significance of pockmarks to understanding fluid flow processes and geohazards. Geofluids 2 (2): 127–136. https://doi.org/10.1046/j.1468-8123.2002.00028.x

Kaul N, Dillon M, Lohrberg A, Nehring F, Plötz A et al. (2023). Sediment echosounder raw data (Innomar SES-2000 working area dataset) of RV ALKOR during cruise AL584, Eckernförde Bay. PANGAEA. https://doi.org/10.1594/PANGAEA.961650

Kim YJ, Koo NH, Cheong S, Kim JK, Chun JH et al. (2016). A case study on pseudo 3-D Chirp sub-bottom profiler (SBP) survey for the detection of a fault trace in shallow sedimentary layers at gas hydrate site in the Ulleung Basin, East Sea. Journal of Applied Geophysics 133: 98–115. https://doi.org/10.1016/j.jappgeo.2016.07.028

Kim YJ, Koo NH, Riedel M, Namgoong H, Lee JM et al. (2017). A case study on swell correction of Chirp sub-bottom profiler (SBP) data using multi-beam echo sounder (MBES) data. Journal of Applied Geophysics 145: 100–110. https://doi.org/10.1016/j.jappgeo.2017.08.001

Kuhn G, Michael EW (1993). Acoustical characterization of sediments by Parasound and 3.5 kHz systems: Related sedimentary processes on the southeastern Weddell Sea continental slope, Antarctica. Marine Geology 113 (3-4): 201-217. https://doi.org/10.1016/0025-3227(93)90018-Q

Labaune C, Tesson M, Gensous B (2005). Integration of high and very high-resolution seismic reflection profiles to study upper Quaternary deposits of a coastal area in the Western Gulf of Lions, SW France. Marine Geophysical Research 26 (2–4): 109–122. https://doi.org/10.1007/s11001-005-3711-z

Mangipudi VR, Goli A (2014). Synthesis of deep multichannel seismic and high-resolution sparker data: Implications for the geological environment of the Krishna–Godavari offshore, Eastern Continental Margin of India. Marine and Petroleum Geology 58: 339–355. https://doi.org/10.1016/j.marpetgeo.2014.08.006

Morelli D, Cuppari A, Colizza E, Fanucci F (2011). Geomorphic setting and geohazard-related features along the Ionian Calabrian margin between Capo Spartivento and Capo Rizzuto (Italy). Marine Geophysical Research 32 (1–2): 139–149. https://doi.org/10.1007/s11001-011-9130-4

Mosher DC, Simpkin PG (1999). Environmental Marine Geoscience 1. Status and trends of marine high-resolution seismic reflection profiling: Data acquisition. Geoscience Canada 26 (4): 174–188.

Nasıf A, Dondurur D (2021). Morphology and potential geohazards using seismo-acoustic data in Sakarya Canyon, Western Black Sea Margin. Geo-Marine Letters 41 (1): 1-11. https://doi.org/10.1007/s00367-021-00688-6

Orange DL, García-García A, McConnell D, Lorenson T, Fortier G et al. (2005). High-resolution surveys for geohazards and shallow gas: NW Adriatic (Italy) and Iskenderun Bay (Turkey). Marine Geophysical Research 26 (2–4): 247–266. https://doi.org/10.1007/s11001-005-3722-9

Pekçetinöz B, Sezgül KM, Eftelioğlu M, Özel E (2009). High-resolution shallow seismic and palynological studies in determining hydrothermal activity in Gülbahçe Bay. Türkiye Jeoloji Bülteni 52 (3): 325-366 (in Turkish with an abstract in English).

Quinn R, Bull JM, Dix JK (1998). Optimal processing of marine high-resolution seismic reflection (Chirp) data. Marine Geophysical Research 20: 13-20. https://doi.org/10.1023/A:1004349805280

Robinson EA, Treitel S (1967). Principles of Digital Wiener Filtering. Geophysical Prospecting 15 (3): 311–332. https://doi.org/10.1111/j.1365-2478.1967.tb01793.x

Saleh M, Rabah M (2016). Seabed sub-bottom sediment classification using parametric sub-bottom profiler. NRIAG Journal of Astronomy and Geophysics 5 (1): 87–95. https://doi.org/10.1016/j.nrjag.2016.01.004

Schock SG, LeBlanc LR, Mayer LA (1989). Chirp subbottom profiler for quantitative sediment analysis. Geophysics 54 (4): 445–450. https://doi.org/10.1190/1.1442670

Shin J, Ha J, Chun JH, Um IK (2022). Field application of 3D CHIRP for geological surveys of shallow coastal regions. Marine Geophysical Research 43 (2): 1-17. DOI: https://doi.org/10.1007/s11001-022-09477-x

Simonetti A, Knapp JH, Sleeper K, Lutken CB, Macelloni L et al. (2013). Spatial distribution of gas hydrates from high-resolution seismic and core data, Woolsey Mound, Northern Gulf of Mexico. Marine and Petroleum Geology 44: 21–33. https://doi.org/10.1016/j.marpetgeo.2013.04.004

Stevenson I, McCann C, Runciman P (2002). An attenuation-based sediment classification technique using Chirp sub-bottom profiler data and laboratory acoustic analysis. Marine Geophysical Research 23: 277–298. https://doi.org/10.1023/A:1025708024518

Subino JA, Dadisman SV, Wiese DS, Calderon K, Phelps DC (2000). Archive of Digital Boomer Seismic Reflection Data Collected Offshore East-Central Florida During USGS Cruise 00FGS01, July 14-22, 2000 (U.S. Geological Survey Data Series No. 496).

Theuillon G, Stephan Y, Pacault A (2008). High-resolution geoacoustic characterization of the seafloor using a subbottom profiler in the Gulf of Lion. IEEE Journal of Oceanic Engineering 33 (3): 240–254. https://doi.org/10.1109/joe.2008.926958

Trabant PK (1986). Applied high-resolution geophysical methods. Offshore Geoengineering Hazards, Springer Dordrecht. https://doi.org/10.1007/978-94-009-6493-8

Vardar D, Alpar B (2016). High-resolution seismic characterization of shallow gas accumulations in the southern shelf of Marmara Sea, Turkey. Acta Geophysica 64 (3): 589–609. https://doi.org/10.1515/acgeo-2015-0059

Vesnaver A, Baradello L (2023). A workflow for processing mono-channel Chirp and Boomer surveys. Geophysical Prospecting 71 (8): 1387–1403. https://doi.org/10.1111/1365-2478.13389

Wu Z, Yang F, Tang Y (2020). High-resolution seafloor survey and applications. Springer Nature Singapore. https://doi.org/10.1007/978-981-15-9750-3

Wunderlich J, Müller S (2003). High-resolution sub-bottom profiling using parametric acoustics. International Ocean Systems 7 (4): 6–11.

Yang Z, Wang X, Hao X, Qian H, Chen X (2022). Research on combined processing techniques of air gun and sparker source towed streamer seismic data. Marine Geophysical Research 43 (2): 1–12. https://doi.org/10.1007/s11001-022-09484-y

Yılmaz Ö (2001). Seismic Data Analysis. SEG Books. https://doi.org/10.1190/1.9781560801580.index

Zheng J, Li L, Xie J, Yan T, Jiang B et al. (2023). The application of a homemade boomer source in offshore seismic survey: From field data acquisition to post-processing. Journal of Applied Geophysics 210: 104945. https://doi.org/10.1016/j.jappgeo.2023.104945